17th AIAA/CEAS Aeroacoustics Conference (32nd AIAA Aeroacoustics Conference)
05 - 08 June 2011, Portland, Oregon

AIAA 2011-2794

Experimental study of flight effects on screech in underexpanded jets

Benoît André*, Thomas Castelain † and Christophe Bailly ‡
Ecole Centrale de Lyon, Ecully, France

Flight effects on screech from an underexpanded supersonic jet have been experimentally investigated by means of a free jet facility. Screech frequency prediction is addressed and some consequences about the convection velocity under flight conditions are drawn. An azimuthal near field acoustic antenna is used to investigate the modal behaviour of screech with forward flight effects. Several mode switchings are spotted while the flight velocity is increased but none can be related to a change in the screech azimuthal mode content. Screech is enhanced by flight at high model jet fully expanded Mach number M_j. This conclusion, deduced from acoustic far field measurements, is supported by Schlieren based analysis. When M_j decreases, it is shown that there exists a decreasing flight velocity limit above which screech eventually fades out.

Nomenclature

c_0	ambient speed of sound
D	model jet nozzle exit diameter
D_j	fully expanded nozzle diameter
f_{acq}	sampling rate
f_s	screech frequency
L_j	shock cell length in Morris' model[1]
L_s	mean shock cell length
m	azimuthal mode order
M_c	convective Mach number
M_f	flight Mach number
M_j	fully expanded jet Mach number
p'_f	filtered fluctuating pressure
p'^s_{rms}	root mean square of screech fluctuating pressure
p'_{rms}	root mean square of total fluctuating pressure
P_{amb}	ambient pressure
P_s	jet static pressure
P_t	jet stagnation pressure
r	radial coordinate
St	fD/U_j
t	time
T_{amb}	ambient temperature

*PhD Student, Université de Lyon, Laboratoire de Mécanique des Fluides et d'Acoustique, UMR CNRS 5509, 36 Avenue Guy de Collongue ; benoit.andre@ec-lyon.fr.

†Assistant Professor, Université Lyon 1, 43 Boulevard du 11 Novembre 1918, 69622 Villeurbanne Cedex ; Laboratoire de Mécanique des Fluides et d'Acoustique, UMR CNRS 5509.

‡Professor, Université de Lyon, Laboratoire de Mécanique des Fluides et d'Acoustique, UMR CNRS 5509, 36 Avenue Guy de Collongue ; Institut Universitaire de France, Paris, France. Senior Member AIAA.

T_s screech time period
T_t jet stagnation temperature
U_c $M_c c_0$
U_f $M_f c_0$
U_j fully expanded jet exit velocity
X axial coordinate
β $\sqrt{M_j^2 - 1}$
γ ratio of specific heats for air
ϕ azimuthal angle
ψ screech phase in a near field pressure signal
θ_e acoustic emission angle
θ_m far field microphone geometrical angle

I. Introduction

Underexpanded supersonic jets usually emit two so-called shock associated noise components beside the mixing noise also present in subsonic jets : the broadband shock associated noise and a tonal noise referred to as screech. Screech has been extensively studied since Powell's work.[2] Powell has explained with some success the generation of this tone by an acoustic feedback loop. In this model, vorticity disturbances originating from the nozzle lip are convected downstream and interact with the shock cell pattern of the jet plume. The acoustic waves emanating from this interaction propagate back to the nozzle where they trigger new disturbances, thus closing the loop. This loop is resonant for some frequencies which are the fundamental screech frequency and the harmonics thereof. For circular jets, Powell[2] isolated four modes, A, B, C and D from the screech frequency evolution with nozzle pressure ratio, defined as the ratio of upstream stagnation pressure to the ambient pressure. Each mode swiching was characterized by a frequency jump. Later, Merle[3] pointed out that the mode A could be divided into modes A1 and A2. Davies & Oldfield[4,5] have subsequently studied the acoustic emission using two microphones located on either side of the jet and have associated the modes with emission patterns. A1 and A2 have thus been classified as being axisymmetric, B sinuous and C helical. Mode D has longer resisted classification but is now known as being sinuous. More recently, Tam *et al.*[6] have proposed a more elaborated model for screech generation based on a description of the relevant turbulent structures as instability waves. The modal characteristics of screech have been studied in detail by Powell *et al.*[7] with measurements of frequency and convection velocity, estimation of source location and focus on the screech unstable behaviour. Along with Ponton & Seiner,[8] they have studied screech modes in light of the jet instability theory and have accredited the instability wave description mentioned above. A summary of the screech knowledge is available in Raman.[9,10]

It has been reported by Hay & Rose[11] that screech could arise on an aircraft in flight and could lead to structural damage. However, as pointed out by Tam,[12] screech in flight has not yet been studied in sufficient details.

The interest in the modifications of jet noise in flight has an evident practical reason and this subject has been addressed on many occasions in the past. The end of the 1970s has thus seen a great effort, both experimental and theoretical, to understand the noise source modifications expected in forward motion. A good summary of this work has been provided by Michalke & Michel[13] who have built an analytical model for mixing noise in flight. In this reference, a discussion on the relevant velocity scale is undertaken in light of some experimental results. Among the early works, Hay & Rose[11] and Bryce & Pinker[14] have addressed the problem of noise from shock containing jets in forward motion. They have proposed an extension of the screech frequency prediction formula to the flight case. This particular problem has been further looked at by Norum & Shearin[15] in connection with pressure measurements in the model jet to assess the effects of forward motion on shock cell length and strength and by Krothapalli *et al.*[16] Norum & Shearin[17] have also addressed the question of screech strength in flight. It can be seen from their results that the screech amplitude is barely modified while the flight Mach number is increased up to 0.4. This conclusion is in agreement with the data of Krothapalli *et al.*[16] but somewhat different from a recent publication by Viswanathan & Czech.[18] The study of Brown *et al.*,[19] where flight Mach numbers go up to 0.8, also suggests a fading of screech at high flight velocities but the tonal emission to the far field seems to be very weak in this work, even under static conditions. Finally, the occurrence of mode switching in flight has been reported by Norum & Shearin[15]

and Norum & Brown.[20] In the former reference, the dominant screech mode between static conditions and $M_f = 0.15$ was seen to switch from C to B for $M_j = 1.67$. Even more, mode C was not found to dominate at any model jet operating conditions with simulated flight. This was later confirmed by Norum & Shearin,[17] where the appearence of new modes at $M_j > 1.55$ has been spotted.

To summarize, few studies have been devoted to screech from jets in forward motion. Moreover, the existing ones usually concentrate on screech frequency prediction. No consensus has been reached on the effect of flight on screech strength and the modal behaviour of screech in flight seems to have only been studied through the analysis of the screech frequency evolution. The present study has been undertaken as a step toward a better understanding of the phenomenon of screech in flight, especially with the aim of addressing these latter two topics.

This paper is organized as follows. First, the experimental facility is presented in Section II and some remarks on the setup influence are made in Section III. Then, the screech frequency prediction for static and forward flight conditions is addressed in Section IV. Flight effects on the screech modal behaviour are investigated in Section V. Finally, effects of forward motion on screech amplitude are identified from acoustic measurements as well as Schlieren based analysis in Section VI.

II. Experimental setup

II.A. The facility

Flight is simulated in the present experiment by a free jet facility, where the model jet is embedded in a larger free flow. In the following, the model jet will also be called primary or supersonic jet while the free jet will also be referred to as secondary or subsonic jet. The jets exhaust in the $10 \times 8 \times 8\,\mathrm{m}^3$ large anechoic room of the Centre Acoustique. The supersonic flow originates from a continuously operating compressor fed with dry air while the subsonic one is generated by a fan system. The model jet is unheated. Within the anechoic room, well upstream of the jet exits, the supersonic duct penetrates into the subsonic flow. In the final section before the exit, both ducts are cylindrical and coaxial. The supersonic duct is maintained at its central position inside the secondary tunnel by a set of 12% thick zero lift airfoil sections. The primary jet exhausts through a 38 mm diameter axisymmetric contoured convergent nozzle of 0.5 mm lip thickness. The results presented herein have been obtained with the secondary duct terminated by a 200 mm diameter round contoured convergent nozzle and both flows have the same exit plane. In the following, the origin of the coordinates is taken at the center of the nozzles. The flow setup can be seen in Fig. 1.

Figure 1. Photograph of the free jet flight simulating facility built in an anechoic environment.

No total pressure probe can be introduced at the end of the primary duct without altering the flow quality. Losses between the regulating valve and the exit plane are here circumvented by measuring the wall static pressure fifteen nozzle diameters upstream of the exit. Stagnation pressure is retrieved from the static pressure value by a local Mach number estimate in the measuring section which is known by the use of the area Mach number relation (see *e.g.* Anderson[21]) with the assumption of a unit exit Mach number. This procedure was tested against nozzle pressure ratio estimates from measured centerline total pressure in the

nozzle exit plane and the agreement was very good. The total temperature of both flows is measured by thermocouple probes. In this paper, model jet operating conditions are given in terms of ideally expanded Mach number M_j being the exit Mach number of a hypothetical perfectly expanded jet operating at the same nozzle presure ratio. In the presented configuration, the extreme operating conditions are $M_j \gtrsim 1.5$ for the model jet and $M_f \gtrsim 0.4$ for the free jet.

The experimental facility has been carefully checked by means of total pressure and hot wire traverses while operating at subsonic conditions to ensure that the flows are axisymmetric from the mean flow and root mean square velocity point of view. Furthermore, the adequacy of the free jet to core jet diameter ratio to simulate flight conditions for shock-associated noise has been verified by measuring the length of the free jet potential core at $M_j = 0.6$ and $M_f = 0.28$. It has been found that the potential core extended up to about $14\,D$. It is to be noted that the secondary potential core length in coaxial arrangements is known not to depend on the inner to outer velocity ratio (see *e.g.* Champagne & Wygnanski[22]). $14\,D$ approximately correspond to eleven shock cells at $M_j = 1.50$ if we assess the mean shock cell length by the formula from Seiner & Norum,[23] $L_s = 1.12\beta D$. Referring to Davies & Oldfield,[4] screech originates primarily from shock cells located further upstream. The part of the shock-containing jet plume which is relevant for screech generation is embedded in the outer flow potential core, and therefore, the free jet to core jet diameter ratio appears sufficient for proper flight simulation. It is to be noted that flight induced shock cell lengthening does not alter this conclusion.

II.B. The measurement techniques

A conventional Z-type Schlieren system has been used to visualize the flow. It consists of a continuous QTH light source, two f/8 parabolic mirrors with diameter of 203.2 mm, a razor blade set perpendicular to the flow direction as filter and a high-speed CMOS camera. The whole system is mounted on an axial traverse which permits the downstream part of the flow to be explored. Far field acoustic data have been obtained from thirteen 6.35 mm diameter PCB condenser microphones fixed on a circular antenna 2020 mm or about $53\,D$ from the centre of the nozzles. The microphones were located every 10° from 30° to 150°. In the following, directivity angles are measured from the downstream jet axis. The transducers were used in normal incidence without protecting grid as is recommended by Viswanathan.[24] The acoustic spectra have been obtained by averaging of 120 individual spectra with frequency resolution of 1 Hz. Near field temporal pressure signals have also been measured by means of a circular antenna laid on the secondary nozzle (see Fig. 2). A similar setup has already been used for the study of screech, for example by Powell *et al.*,[7] Ponton & Seiner[8] or Massey & Ahuja.[25] Such an arrangement is essential to study screech modes from the phase relations between the microphones. Depending on the case considered, 15 or 18 PCB microphones are located on a 18-holes circular mesh with 20° azimuthal periodicity. All pressure signals were acquired at a rate of 102400 Hz by a National Instrument PXI 5733 board.

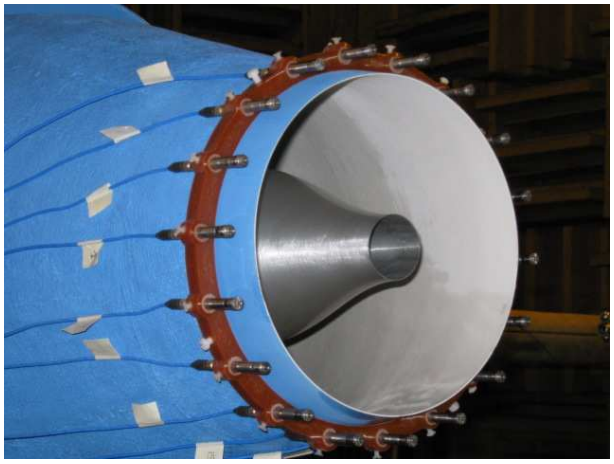

Figure 2. The circular near field antenna used for screech mode study.

III. Preliminary remarks on the setup influence

III.A. Presence of the secondary nozzle

The evolution of screech frequency with supersonic jet Mach number without simulated flight ($M_f = 0$) has been measured both with and without secondary nozzle. In the latter case, the secondary duct finished off 0.5 m upstream of the nozzle exit plane. The results are shown in Fig. 3 where only fundamental frequencies are displayed. The general Mach number dependence of screech frequency is very similar to the well known evolution, see *e.g.* Powell *et al.*[7] Several modes can readily be spotted. The main difference between the two configurations considered here consists in the behaviour of screech at $M_j > 1.4$. With secondary nozzle, the mode switching from B to the upper mode takes place at $M_j = 1.44$ and contrary to the expected evolution, the jump occurs to lower frequencies. It is believed that the upper mode is b after the nomenclature of Powell *et al.*[7] where this mode was defined as being the persistence of mode B in a M_j range where the helical mode C of higher frequency was prominent. Here however, we see a slight jump in the frequency curve from mode B to mode b, which was as well clearly audible during the tests. This feature usually tends to pinpoint a mode switching. But still, the mode above $M_j = 1.44$ will be referred to as mode b in the following and its characteristics will be addressed in a later section. Without secondary nozzle however, a similar jump occurs at $M_j = 1.41$ while at slightly higher jet Mach numbers, screech is unstable between two distinct modes, the upper one being probably the expected C mode of higher frequency. Furthermore, the intricate mode A2 is different between the two secondary nozzles. Hence, the experimental assembly alone has already an effect on screech. It has to be noticed that apart from these discrepancies, screech frequencies are equal for a given jet Mach number.

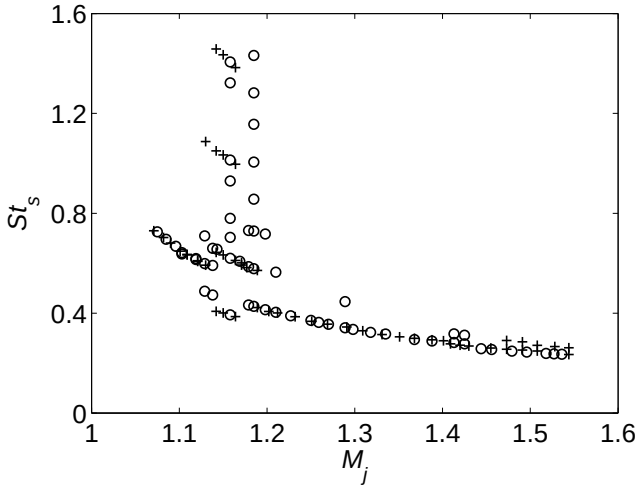

Figure 3. Evolution of Strouhal number based on screech frequency (St_s) with jet Mach number M_j without flight effect ($M_f = 0$). + no secondary nozzle ; ○ with secondary nozzle.

III.B. Mach number and static pressure profiles in the secondary flow

Total and static pressure measurements have been performed in the secondary jet at several values of the fan engine speed with $M_j = 0$, from which a local Mach number has been computed. The results are displayed in Fig. 4. It is apparent that the Mach number is not uniform across the secondary flow, which decelerates toward the core jet. This variation is entirely due to the static pressure profile since total pressure (not shown here) is constant. The static pressure increase toward the inner jet can be attributed to the free jet curvature which is imposed by the primary nozzle. A test has been performed with a truncated convergent secondary nozzle whose exit plane is located about $3.6\,D$ upstream of the model jet exit. In this case as well, where the secondary flow has a free outer mixing layer prior to the primary jet exit plane, the same effect on P_s has been observed. It is worth noting that some radial profiles of axial velocity by Plumblee[26] clearly show the same feature, although the secondary stream was a large scale wind tunnel in this work. This last remark, along with the test performed with truncated secondary flow nozzle, tends to pinpoint that the outer shape of the model jet nozzle alone is the cause for the static pressure profile. This effect raises an

important question on the actual fully expanded jet Mach number M_j set for a given test. If the upstream total pressure P_t is maintained at the value calculated to provide the targeted M_j while increasing M_f, the actual M_j should decrease during the test due to the increased static pressure sensed by the model jet at the nozzle exit. This would call for an adjustement of P_t during the course of the experiments. However, it is believed that the same kind of ambient static pressure evolution should exist on the full scale problem due to the form of the engine cowl. As a consequence, no P_t adjustement has been performed during the flight tests and the relevant value of total pressure has been calculated from the ambient pressure at $M_f = 0$.

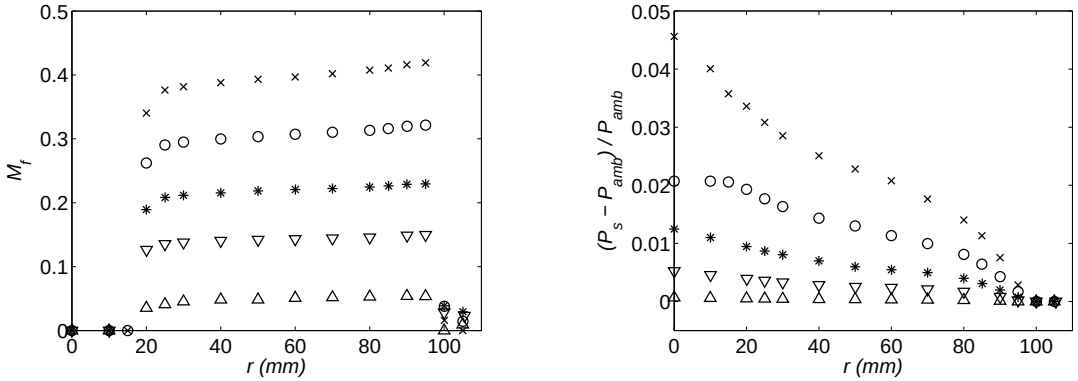

Figure 4. Local flight Mach number M_f (left) and static pressure P_s (right) transverse profiles at $X = D/2$. Fan engine speeds are denoted by the power supply related to its maximum value : △ 11%, ▽ 30.5%, * 47%, ○ 66%, × 86%. The primary jet ($r < 19$ mm) is not operated ($M_j = 0$).

Fan engine speeds have been translated into values of M_f by means of a calibration procedure where the local Mach number has been measured approximately at the center of the free jet. It appears then that this value must be taken as a mean rather than as a unique M_f characterizing the secondary flow.

To finish with, Morris[27] already pointed out the influence of the upstream boundary conditions in a dual stream flow setup. He measured a non-linear dependence of the peak axial turbulence intensity on velocity difference between both streams and attributed it to the influence of upstream velocity profile, which persists far downstream of the jet exit. He also stated that the non-linear dependency should be peculiar to each experimental assembly. The feature mentioned above is believed to be one of these effects that should be facility dependent.

IV. Screech frequency in static and flight conditions

IV.A. Static case

Powell[2] has explained screech as being the effect of an acoustical feedback loop. This mechanism has allowed him to develop a screech frequency prediction formula. According to that model, the screech temporal period is the sum of the time taken by flow disturbances to travel down one shock cell and of the time needed by the acoustic waves outside the jet to propagate back the same distance toward the nozzle. This can be written as

$$T_s = L_s/U_c + L_s/c_0 \tag{1}$$

Equation (1) leads straightforwardly to the expression of the screech frequency f_s

$$f_s = U_c/[L_s(1 + M_c)] \tag{2}$$

Such a formula does not predict the different modes. Depending on the retained expressions for L_s and U_c as a function of M_j and jet total temperature T_t, many final expressions for f_s have been proposed in the past. The evolution of L_s with M_j has been the subject of a number of experimental and theoretical studies. The reader is referred to the review by Powell.[28] The shock cell lengthening with M_j has in general been expressed as a function of βD. The example of Seiner & Norum[23] has already been quoted, who write $L_s = 1.12\beta D$. The convection velocity is usually written as a fraction of the jet fully expanded velocity U_j. $U_c = 0.7\,U_j$ seems to be the most usual value. However, Panda *et al.*[29] report some convection velocity measurements for each screech mode of a circular nozzle and have found a significant variation with the mode.

Theoretically, Tam *et al.*[6] explain screech as the interaction between large scale structures and shock cells. The frequency is said to be determined by the weakest link of the feedback loop and essentially the same expression as that of Eq (2) is found. The frequency expression has been rewritten to express $f_s D_j/U_j$ as a function of M_j and T_t only, as

$$\frac{f_s D_j}{U_j} = \frac{0.67}{(M_j^2-1)^{1/2}}\left[1+0.7M_j\left(1+\frac{\gamma-1}{2}M_j^2\right)^{-1/2}\left(\frac{T_{\rm amb}}{T_t}\right)^{-1/2}\right]^{-1} \tag{3}$$

Massey & Ahuja[25] have proposed two different screech formulæ for mode A and C, starting from Eq. (3) and using more precise U_c estimates for each mode. Also, it was noticed that a $(M_j^2-1)^{1/3}$ dependence of shock spacing allowed a better fit of the experimental data. In this reference, f_s for mode A is written as

$$\frac{f_s D_j}{U_j} = 1.25\,\frac{0.63}{1.1(M_j^2-1)^{1/3}}\left[1+0.63M_j\left(1+\frac{\gamma-1}{2}M_j^2\right)^{-1/2}\left(\frac{T_{\rm amb}}{T_t}\right)^{-1/2}\right]^{-1} \tag{4}$$

and for mode C (helical) as

$$\frac{f_s D_j}{U_j} = \frac{0.615}{1.1(M_j^2-1)^{1/3}}\left[1+0.615M_j\left(1+\frac{\gamma-1}{2}M_j^2\right)^{-1/2}\left(\frac{T_{\rm amb}}{T_t}\right)^{-1/2}\right]^{-1} \tag{5}$$

The Strouhal numbers $St_s = f_s D/U_j$ computed from these expressions are superimposed on our measured values in Fig 5. The ordinate axis has been magnified as compared to Fig. 3 to facilitate visualization. Along with the mode A and C predictions is plotted a formula for mode B constructed after Massey & Ahuja, which was left out by these authors. This expression writes as follows

$$\frac{f_s D_j}{U_j} = \frac{0.58}{1.12(M_j^2-1)^{1/3}}\left[1+0.58M_j\left(1+\frac{\gamma-1}{2}M_j^2\right)^{-1/2}\left(\frac{T_{\rm amb}}{T_t}\right)^{-1/2}\right]^{-1} \tag{6}$$

where the estimate $U_c = 0.58\,U_j$ is taken from Panda *at al.*[29] for mode B. It can be seen that the agreement is good for all modes. The formula of Massey & Ahuja[25] for mode A seems in particular to be calibrated for mode A2. Eq. (5) is in agreement with the few higher frequency points without secondary nozzle at high Mach number, thus confirming that this mode is indeed the expected helical mode. Finally, Eq. (6) follows closely the measured frequencies for mode B over a large M_j range, giving support to the $(M_j^2-1)^{1/3}$ dependence of shock spacing proposed by Massey & Ahuja.

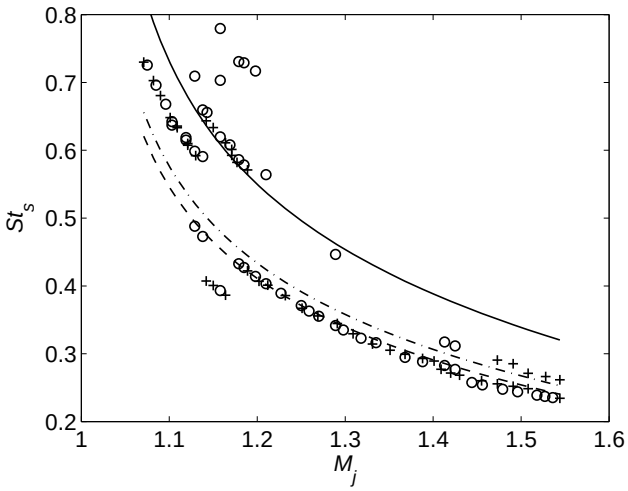

Figure 5. Measured St_s against M_j, $M_f = 0$. + no secondary nozzle ; ○ with secondary nozzle. — Eq. (4), −− Eq. (6), −·− Eq. (5).

IV.B. Flight configuration

A detailed survey of the screech modes observed has been performed and M_j values of 1.10, 1.15, 1.35 and 1.50 have been selected. According to the screech literature and the discussion reported in section III.A, these fully expanded Mach numbers correspond to mode A1, A2, B and b respectively. For these fixed values of M_j, M_f has been varied gradually from 0 to about 0.4 upward and downward. Time signals of one or two seconds have been recorded by the microphones located in the near field, on the azimuthal antenna shown in Fig. 2. From these signals, the screech frequency evolution with M_f has been calculated and the results are displayed in Fig. 6 (a), (b), (c) and (d) for mode A1, A2, B and b, respectively. One can see that the screech frequency has a general tendency to decrease in flight. In all cases, and especially for $M_j = 1.15$, the frequency evolution is discontinuous. Finally, some frequency jumps are seen to give raise to hysteretical behaviours, insofar as the upward and downward frequency curves are not always superimposed. The labels in Fig. 6 pertain to the study developed in Sec. V. The screech frequency prediction in flight is now discussed.

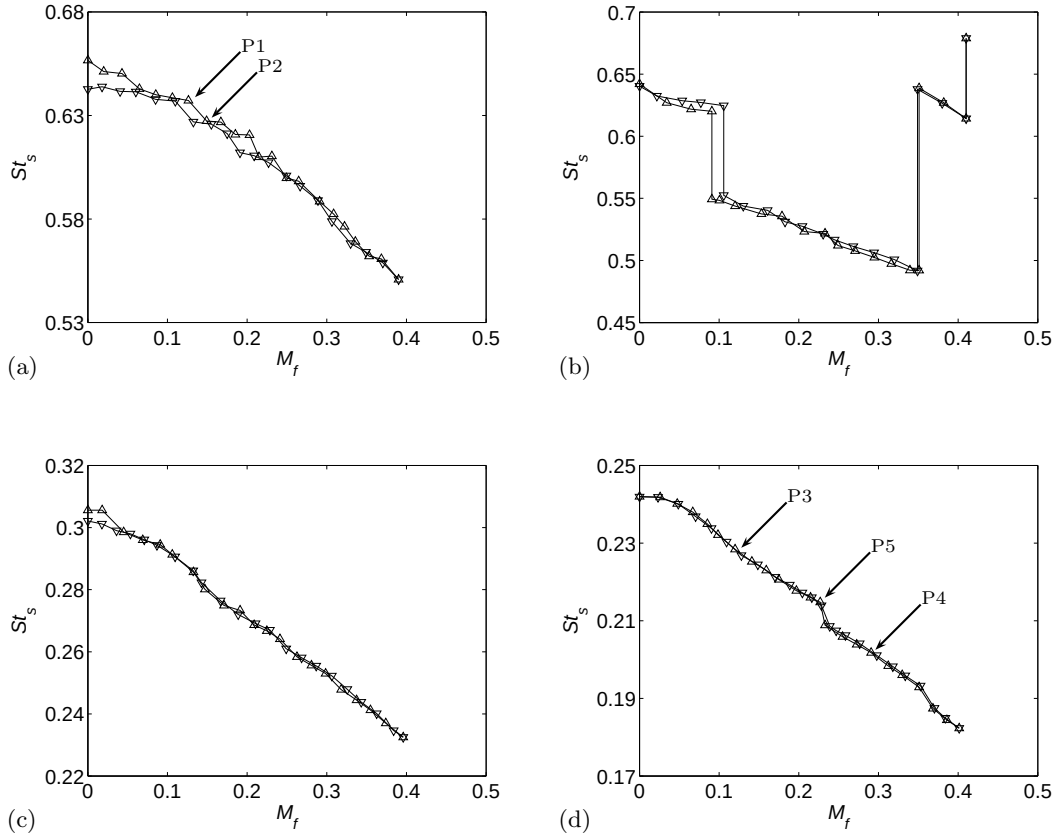

Figure 6. Evolution of St_s with flight Mach number. (a) mode A1, M_j = 1.10 ; (b) mode A2, M_j = 1.15 ; (c) mode B, M_j = 1.35 ; (d) mode b, M_j = 1.5. △ upward evolution of flight velocity ; ▽ downward evolution of flight velocity.

Point name	M_j	M_f	M_f direction
P1	1.10	0.13	upward
P2	1.10	0.15	upward
P3	1.50	0.12	upward
P4	1.50	0.29	upward
P5	1.50	0.23	upward

Table 1. Description of the points studied specifically in Sec. V.

The screech frequency prediction formula has been extended to forward flight by Hay & Rose[11] starting from Powell's[2] static expression. Basically the same analysis has been later performed by Bryce & Pinker.[14] The only modification of the screech time period expression in flight as compared to Eq. (1) arises from

the slowed acoustic propagation back toward the nozzle, which explains the observed frequency drop with increasing M_f. Similarly to Eq. (1), one can write

$$T_s = L_s/U_c + L_s/(c_0 - U_f) \tag{7}$$

This leads to

$$f_s = U_c/(L_s[1 + M_c/(1 - M_f)]) \tag{8}$$

Equation (8) is also the same as that given by Tam.[12] Here again, the relevant expressions for L_s and U_c can be discussed. First, the importance of considering the shock cell lengthening for frequency prediction has already been pinpointed by Norum & Shearin.[15] Morris[1] has proposed an expression for the shock cell length in flight from a vortex sheet model with proper boundary conditions. From $L_j \propto \beta D_j$ calculated in Morris,[1] L_s is computed as $L_s = L_j\, D/D_j$. The prediction of shock cell lengths with forward motion is shown in Fig. 7 for $M_j = 1.50$ along with some measurements from Schlieren recordings of the present study. Also displayed are mean shock cell lengths estimates from static pressure profiles of Norum & Shearin[30] for $\beta = 1.10$, or $M_j = 1.49$. The agreement between the theory and the present results is seen to be good, especially considering the dispersion in the experimental data.

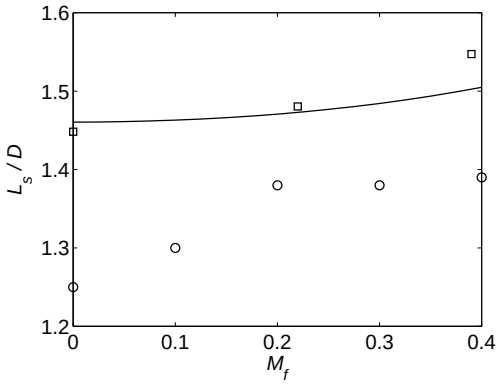

Figure 7. Shock cell length L_s normalized by the nozzle diameter D as a function of M_f. □ present study, $M_j = 1.5$, ○ Norum & Shearin,[30] $\beta = 1.10$. — Morris' model.[1]

As for the convection velocity, Bryce & Pinker propose to write $U_c = 0.7\,(U_j - U_f) + U_f$ as an adaptation of the static formula. This can be adjusted by replacing 0.7 by α and make it vary for each screech mode according to the measurements of Panda *et al.*[29] Moreover, the subject of convection velocity in dual stream flows has recently been studied by Murakami & Papamoschou[31] and an expression for U_c has been formulated in the case of a shock-free supersonic core jet with a subsonic outer jet. Finally, the study of Sarohia & Massier[32] suggests that the boundary layer on the engine cowl, or for us on the outer side of the model jet nozzle, shields the model jet from the secondary flow and makes the relevant velocity in the mixing layer U_j and not $U_j - U_f$. Hence, according to this,

$$U_c = \alpha\, U_j. \tag{9}$$

The three prediction formula for f_s derived from these expressions for U_c have been tested against the measured screech frequency displayed in Fig. 6 for the two higher Mach number cases. The results are depicted in Fig. 8, for $\alpha = 0.58$ coming from Panda *et al.*[29] and L_s coming from Morris' model.[1] It is visible that the values of St_s calculated with U_c of Murakami & Papamoschou are the furthest off the measurements. Between the two others U_c expressions, Eq. (9) leads to a better prediction of the slope of St_s with M_f. In fact, the agreement is very good for both M_j if one matches the predicted Strouhal number to the measured one at $M_f = 0$. This would support the hypothesis of Sarohia & Massier.[32]

V. Analysis of near field microphone signals

In addition to screech frequency calculations, the time signals have also been used to study the modal behaviour of screech in flight. Several analyses have been performed. The first one is associated with the localization of the plane of antisymmetry for sinuous screech modes. The screech amplitude sensed by a microphone in the near field next to the plane azimuthal location is vanishing while it is maximum for

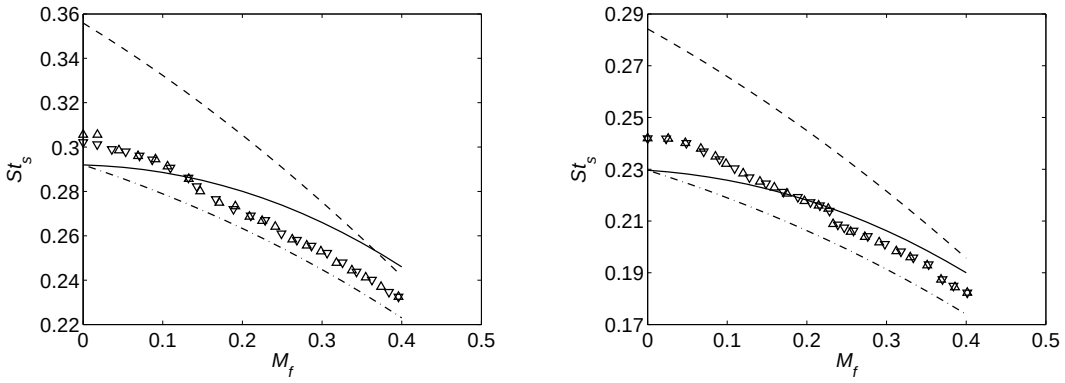

Figure 8. Predictions of screech frequency in flight by Eq. (8). Left : $M_j = 1.35$, right : $M_j = 1.50$. L_s is computed as in Morris.[1] $\triangle$, $\triangledown$ measurements, — $U_c = 0.58\,(U_j - U_f) + U_f$, -- U_c from Murakami & Papamoschou,[31] $-\cdot-$ $U_c = 0.58\,U_j$.

microphones located 90° to the plane. Moreover, this mode is known to rotate.[7] This behaviour can thus be followed in time by tracking the azimuthal location of the lowest root mean square pressure calculated over a small number of screech periods, *i.e.* ten in the results presented here.

Second, the phase relationships between the microphones have been estimated in the following manner. One near field microphone has been chosen as phase reference and its azimuthal angle ϕ is taken as 0° arbitrarily. For each of the remaining microphones, the phase angle difference to the reference microphone has been computed from the time delay yielding the maximum cross-correlation between the two time signals. Ten screech periods have been considered for computing the cross-correlations. Repeating the calculation for such blocks of screech periods over the whole duration of the signals has allowed the time evolution of phase differences to be followed. To ensure that no erroneous points are taken into account, the calculated phase relations are rejected when the associated maximum coefficient of correlation is below 0.75.

Third, the modal detection technique by Massey & Ahuja[25] has been implemented and used to check some of the time results. It delivers a measure of the modal amplitude associated with each azimuthal mode contained in the time signals. Contrary to the other two techniques, this one provides a time integrated result.

Before applying the first two processings, the time signals have been digitally filtered around the screech frequency to achieve cleaner results. The attenuations in the stopbands have been set as small as possible to alleviate phase shifting by the filter. It was checked that the phase shift was small by plotting the angle of the spectra around f_s for filtered and unfiltered signals. In the following, only a few points are discussed for the cases $M_j = 1.10$ and 1.50. They are labeled on the frequency plots of Fig. 6 and described in Table 1.

V.A. Mode A1

The case of $M_j = 1.10$ is discussed in what follows. The screech Strouhal number evolution against M_f is shown in Fig. 6 (a) and some small discontinuities can be spotted. Some results associated with the one occurring around $M_f = 0.13$ are considered now and displayed in Fig. 9. A time trace of P1 is shown in Fig. 9 (a). All microphones are seen to be in phase on this sample. The modal detection (b), which is an integrated result over the one-second recording, confirms that the axisymmetrical mode $m = 0$ dominates over the helices $m = \pm 1$. Fig. 9 (c) and (d) depict the result of the phase relation calculations for P1 and P2. The phase relation $\Delta\psi$ is written as a fraction of screech frequency. Thus, $\Delta\psi = 0$ means that the signals are in phase, while $\Delta\psi = \pm 0.5$ stands for an opposite phase relation. It is visible that both points correspond to an axisymmetrical mode since all microphones are approximately in phase throughout the whole recording. It should be noted that the calculated phase relations $\Delta\psi$ can only take discrete values due to the signal discretization. The resolution is f_s/f_{acq}, where f_{acq} is the sampling rate. For the case in Fig. 9 (c), it amounts to 0.057 screech periods, which explains that the displayed phase relations are not quite smooth. A detailed survey of all recordings allows us to conclude that the screech mode remains axisymmetrical at all M_f values.

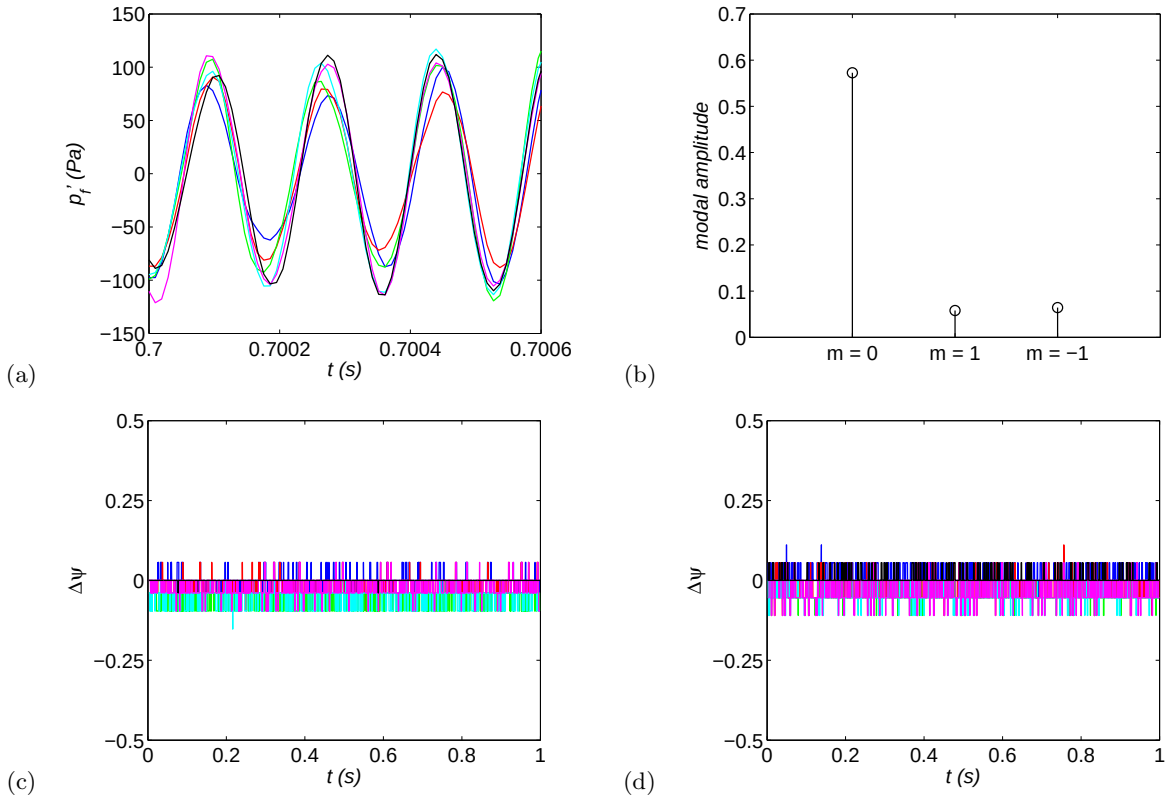

Figure 9. Mode A1, $M_j = 1.10$. Point P1 : (a) time signals ; (b) modal content ; (c) phase relations $\Delta\psi$ against time. Point P2 : (d) $\Delta\psi$ against time. — $\phi = 40°$, — $\phi = 100°$, — $\phi = 160°$, — $\phi = 220°$, — $\phi = 280°$, — $\phi = 340°$.

V.B. Mode b

The upper fully expanded Mach number investigated was $M_j = 1.50$. The screech frequency evolution is displayed in Fig. 6 (d) and a small jump occurs around $M_f = 0.23$. The phase relations for P3 on one side of the jump and P4 on the other side are shown in Fig. 10. This mode is obviously flapping since the microphones can be gathered into two groups which are in opposite phase relations. In fact, the screech is always flapping away from the frequency jump, which does thus not change the selected screech mode. Incidentally, these results confirm that this upper mode of screech is indeed a mode b as it was stated earlier, and not a mode C.

Point P5 is nevertheless worth mentioning. This recording is the one right before the frequency jump to lower frequencies. The position of the rotating plane of antisymmetry is shown in Fig. 11 (a) over a short time period extracted from the 1-second recording while the phase relations are displayed in (b) over the same time interval. Moreover, the time traces (not shown here) very much look like the ones shown by Powell *et al.*[7] in their Fig. 15 (a), revealing rapid and strong amplitude modulations over time. The plane rotation and the phase relation motive are both fully stationary throughout the whole recording. The phase relation pattern looks rather puzzling at first sight but has been artificially reconstructed in the following manner. First, it was observed that the plane completes approximately forty half-rotations in the second, which corresponds to two screech frequencies 41 Hz apart visible in the acoustic spectra (not shown here). Furthermore, the modal detection algorithm shows very clearly that one frequency contains exclusively the azimuthal mode $m = -1$ while the other one contains $m = +1$. In order to build artificially the two helices, their respective amplitudes have been found by filtering sharply around each peak frequency and noting the amplitude of the resulting p'_f signal. The ratio of these two amplitudes is the relevant parameter to properly reconstruct the time signals. Finally, the phase relation calculation has been applied to the artificial signal made up of both helices and the pattern shown in Fig. 12 has been obtained. It is obviously the same pattern as in the experimental counterpart. One can thus conclude that the screech at P5 is made up of two counter-rotating helices of different frequencies and amplitudes. Incidentally, this agreement demonstrates the adequacy of the whole procedure. It was observed that this peculiar behaviour builds up from the three

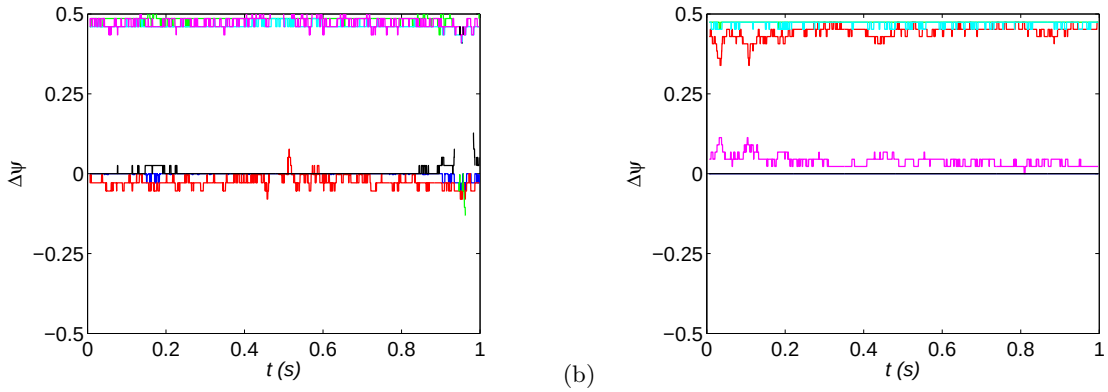

Figure 10. Phase relations $\Delta\psi$ against time. Mode b, $M_j = 1.50$. (a) P3 ; (b) P4. — $\phi = 40°$, — $\phi = 100°$, — $\phi = 160°$, — $\phi = 220°$, — $\phi = 280°$, — $\phi = 340°$.

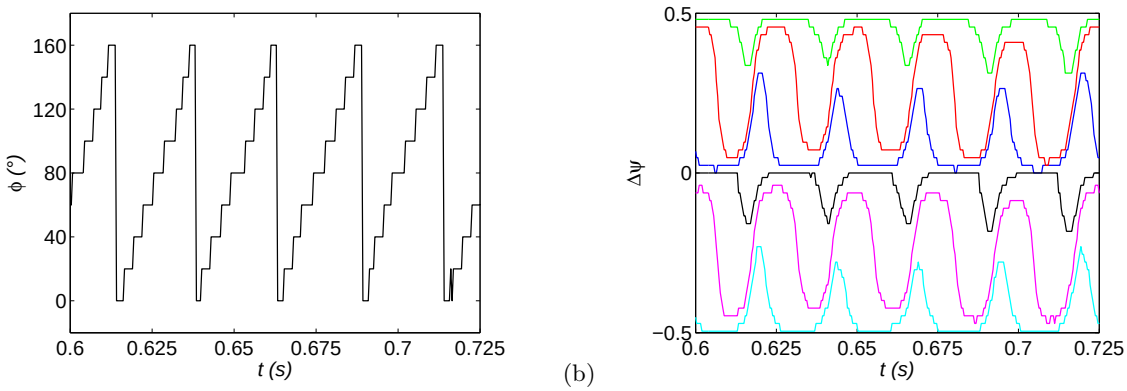

Figure 11. Mode b, $M_j = 1.50$, P5. (a) location of the plane of antisymmetry over one eighth of a second ; (b) phase relations $\Delta\psi$ in the same time interval. — $\phi = 40°$, — $\phi = 100°$, — $\phi = 160°$, — $\phi = 220°$, — $\phi = 280°$, — $\phi = 340°$.

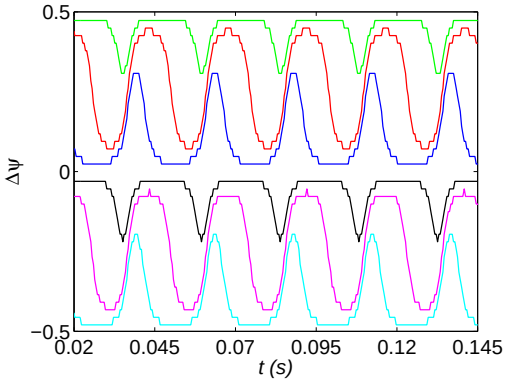

Figure 12. Reconstruction of the phase relations for a time signal containing : $m = +1$ at a frequency $f = 2462$ Hz and an amplitude of 1200 Pa ; $m = +1$ at a frequency $f = 2421$ Hz and an amplitude of 800 Pa. 2421 Hz and 2462 Hz are the two frequencies arising for point P5. — $\phi = 40°$, — $\phi = 100°$, — $\phi = 160°$, — $\phi = 220°$, — $\phi = 280°$, — $\phi = 340°$.

previous points at lower M_f and completely vanishes just after the jump. Interestingly, exactly the same pattern is visible for the branch from $M_f = 0.4$ downward after the jump. One could have been tempted to explain the first jump toward lower frequencies when M_f is increased by a screech that had become unstable due to forward flight. However, the jump toward higher frequencies on the way back to $M_f = 0$ seems to deny this hypothesis. Indeed, the lower frequency branch should then have shown some similar signs of instability *before* the second jump, and not *after*. The reason for such a frequency discontinuity remains ellusive.

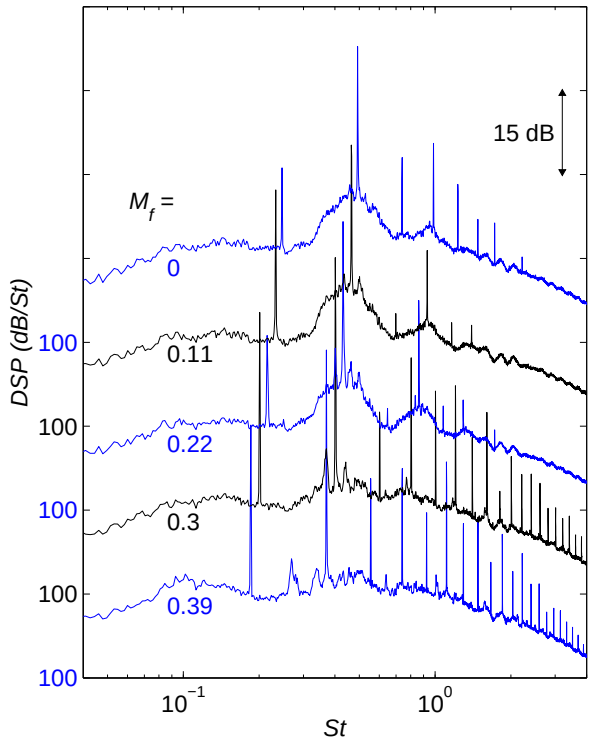

Figure 13. Far field acoustic spectra in dB/St, with $St = fD/U_j$. $M_j = 1.50$, $M_f = 0.$, 0.11, 0.22, 0.30, 0.39. $\theta_e = 90°$.

VI. Flight effects on screech amplitude

VI.A. Far field acoustic results

One well-known disadvantage of free jet facilities to simulate flight conditions is the presence of the external shear layer between the secondary jet and the quiescent medium, non existent in a real flight configuration, and whose influence on the radiated sound waves must be eliminated. Many studies have addressed this issue in the past and the correction procedures are now widely accepted. The angle correction used in this study comes from Amiet,[33,34] and is the same as in Ahuja *et al.*[35] Spectra at equal emission angle θ_e are compared since this angle should reflect source changes due to flight and not spectral modifications due to propagation effects. Amiet's amplitude correction for a cylindrical shear layer[34] has also been implemented. The correction to equal distance from the present source position has been retained, *not* the correction to equal distance from what is referred to as the retarded source position in this reference. No account has been taken for the actual source position : the source is supposed to be located at the nozzle exit for angle and amplitude corrections.

The cases $M_j = 1.10$, 1.35 and 1.50 are now investigated specifically. These values of M_j correspond to modes A1, B and b. A2 is not included because of the significant flight induced mode switches reported above, which could have made any comparison throughout the M_f range tentative. Only data for $\theta_e = 90°$ are shown. At this angle, θ_e is very near the geometrical angle θ_m and amplitude corrections are small. $\theta_e = 37.5°$ and 130° have also been investigated and lead to the same conclusions as the ones presented here. Some spectra are displayed in Fig. 13 for $M_j = 1.5$ and $\theta_e = 90°$. It is already apparent that the screech does not abate at high M_f, which is at odds with the conclusion of Viswanathan & Czech.[18] To the contrary, it seems rather enhanced as is visible from the number of harmonics that appear. In order to account for the large number of harmonics, the far field spectra are analysed as follows. The overall sound pressure level (OASPL) for the corrected spectra are computed. Then, the screech peaks are digitally removed and the power spectral density linearly interpolated over the defined narrow gaps. A screech free spectrum is thus built, whose OASPL is also calculated. From these two OASPLs, the sound pressure level pertaining to screech exclusively can be deduced by subtraction. This sound pressure level, noted SPL_s, contains the contribution of all screech harmonics and its evolution with M_f shows directly the total screech energy

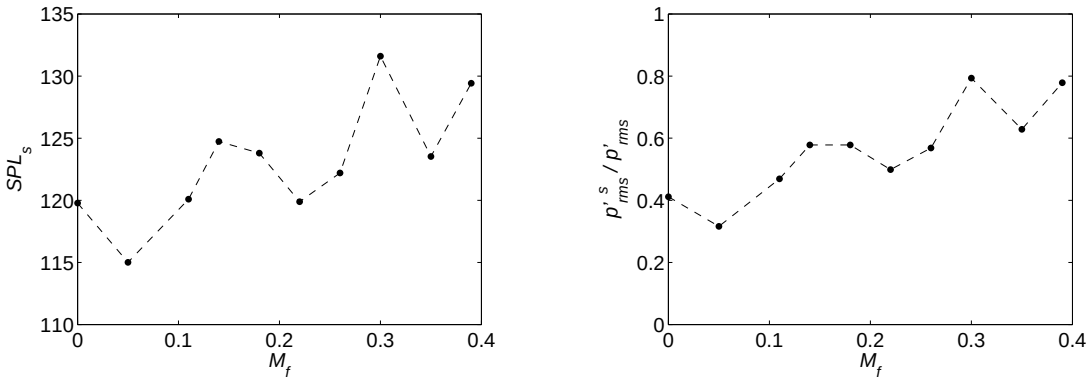

Figure 14. Left : evolution of screech sound pressure level with flight Mach number M_f. Right : screech energy fraction against M_f. $M_j = 1.50$, $\theta_e = 90^\circ$.

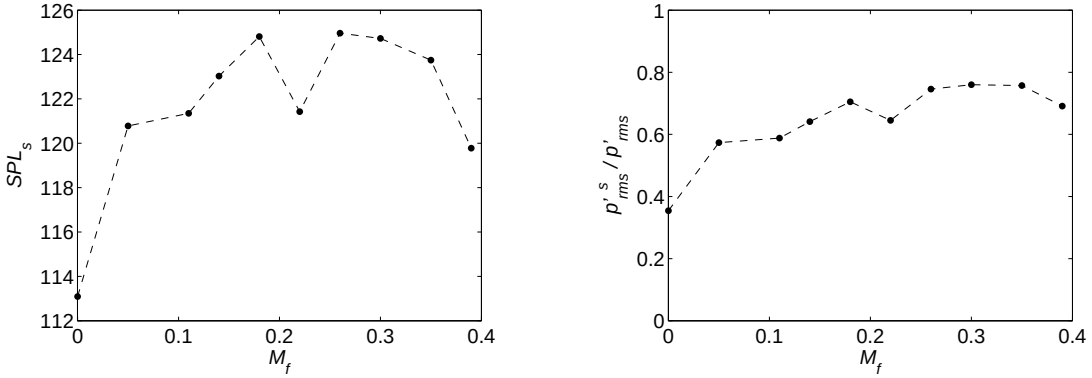

Figure 15. Left : evolution of screech sound pressure level with flight Mach number M_f. Right : screech energy fraction against M_f. $M_j = 1.35$, $\theta_e = 90^\circ$.

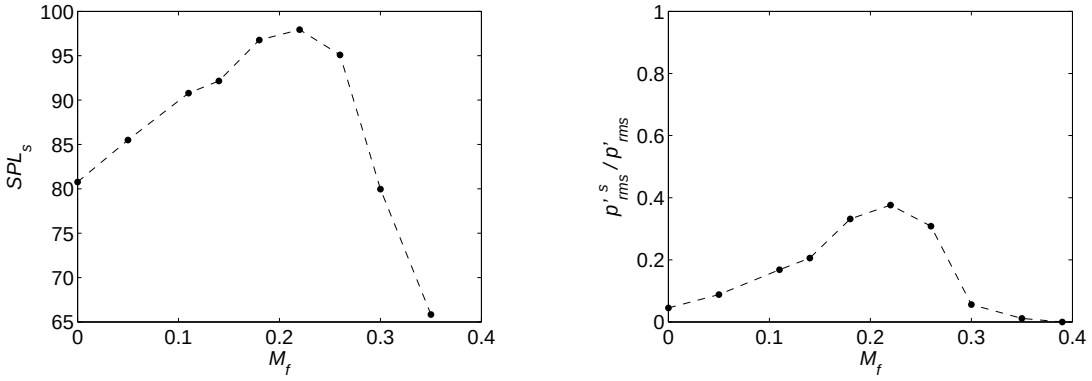

Figure 16. Left : evolution of screech sound pressure level with flight Mach number M_f. Right : screech energy fraction against M_f. $M_j = 1.10$, $\theta_e = 90^\circ$.

dependence on flight Mach number. From the OASPL of the complete spectrum and $\mathrm{SPL_s}$, the portion of the total acoustic energy coming from screech, $p'^{s}_{\mathrm{rms}}/p'_{\mathrm{rms}}$, can ultimately be calculated. This procedure presents also the advantage of considering a possible widening of the screech peaks which could arise from turbulence scattering by the external shear layer, as discussed in Schlinker & Amiet.[36] It is believed the whole screech energy is thus considered, apart from what is lost by turbulence absorption through the external shear layer.

Some results are shown in Fig. 14 for $M_j = 1.50$. The OASPLs have been computed for $f > 500\,\mathrm{Hz}$ to avoid considering the low frequency range where reflections could occur. Above this frequency, it was checked for all directivity angles that the noise radiated by the external shear layer of the secondary flow is insignificant

compared to the noise from the model jet. Although the curves are not monotonous, the conclusion drawn from the spectra displayed in Fig. 13 is confirmed. SPL_s is globally increasing as M_f grows. Furthermore, the portion of acoustic energy coming from screech is also increasing and reaches about 0.8 above $M_f = 0.3$, which is twice the screech content at $M_f = 0$.

The case $M_j = 1.35$ is shown in Fig. 15. A global increase of SPL_s with M_f is also to be noted. The screech energy portion doubles between $M_f = 0$ and 0.30. However, the levels drop slightly at the higher flight Mach numbers.

In the $M_j = 1.10$ case, the cutoff frequency for computing OASPLs had to be raised to 1500 Hz due to the lower model jet noise levels. Above it, the noise radiated by the external shear layer is at least 7 dB/Hz beneath the core jet noise. Here, the conclusions are different from the two cases mentioned above, as shown in Fig. 16. While M_f is increasing, the screech is also enhanced but reaches maximal strength at $M_f = 0.22$ before dropping and extinguishing at last at $M_f = 0.39$. Considering all the M_j cases analysed, one may conclude that there exists a M_f-limit for all M_j above which screech is finally reduced and that this limit increases with M_j. According to this hypothesis, $M_f = 0.39$ would not be high enough for the screech levels at $M_j = 1.5$ to fade out.

VI.B. Indirect observation of screech behaviour at high flight velocity

The enhancement of screech by flight Mach number at high M_j has also been spotted through indirect effects of screech on the underexpanded jet dynamics. A collage made out of three spark Schlieren images for the case $M_j = 1.50$ and $M_f = 0.39$ is shown in Fig. 17. The attention is drawn on two features visible in this figure : the first shock is seen to be twisted within the jet plume, denoting a strong oscillation amplitude, and a large flapping motion of the jet occurs further downstream. The latter feature is now specifically addressed.

Sarohia *et al.*[37] have reported a large scale lateral oscillation of the supersonic jet in simulated flight conditions, also termed whipping motion in this reference. Other shadowgrams by Sarohia[38] clearly show this feature. Furthermore, Sarohia *et al.*[37] have suppressed screech by inserting a rod inside the jet plume but could still observe the whipping motion, from which they have inferred that it is not related to screech. In the case of Fig. 17, the oscillation amplitude has been roughly estimated to be of the order of one jet diameter. A pattern tracking procedure has been developed by the authors.[39] This procedure permits one particular pattern to be followed from frame to frame in a recorded movie obtained by the Schlieren setup. The application of this algorithm to the jet boundary has permitted the flapping frequency to be extracted and it was seen that the jet flaps at the screech frequency, pleading for a connection between this motion and the tonal emission. With no flight velocity however, no obvious flapping is visible although screech is present. Consequently, it may as well be the screech enhancement by the simulated flight which generates the strong whipping motion. This would corroborate the conclusion drawn from the far field acoustic results.

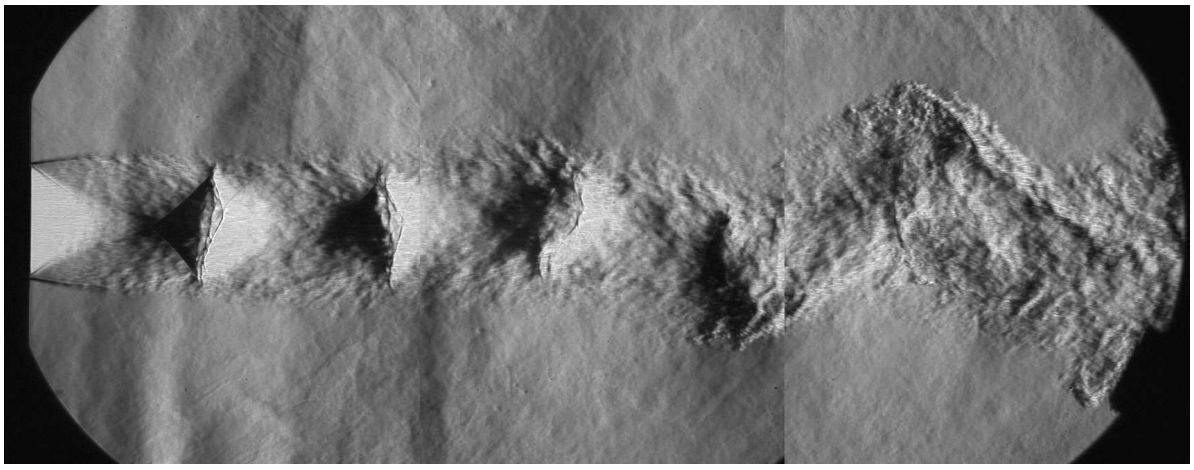

Figure 17. Collage from three spark Schlieren pictures of the supersonic jet plume. $M_j = 1.50$, $M_f = 0.39$. Exposure time is 6.7 μs.

VII. Conclusions

Flight effects on screech from an underexpanded supersonic jet have been experimentally investigated by means of a free jet facility. Near field and far field acoustic measurements have provided some insight into the behaviour of screech amplitude and frequency under flight conditions and have been supplemented by Schlieren visualizations. The near field measurements have been performed with a circular antenna mounted on the secondary nozzle.

It was shown that the experimental setup alone had some effects on the screech modes, thus confirming the screech sensitivity to boundary conditions. Furthermore, a non homogeneous free jet has been observed, which seems inherent to the flight simulation setup. More specifically, a static pressure increase in the outer jet cross section toward the model jet has been pinpointed. However, it is believed that such a behaviour should also arise in the full scale problem.

The far field acoustic results have been analysed in a way that permits all the acoustic energy associated with screech to be considered, by including not only the fundamental tone but also the numerous harmonics. From $M_j = 1.10$ to 1.50, the results are found consistent. It is seen that screech is enhanced by forward motion up to a particular flight velocity, after which it is eventually reduced. This effect is obvious for $M_j = 1.10$, where screech disappears at high flight Mach number. It is less evident for $M_j = 1.35$ and rather not visible for the higher M_j of 1.50. It is possible that still higher flight Mach number are required for the screech at $M_j = 1.50$ to fade out. The screech enhancement by flight velocity in the higher M_j case has also been spotted through screech effects on the model jet dynamics. In particular, the jet large scale whipping motion occurring at high flight Mach number has been related to screech and its amplitude was seen to be emphasized at higher M_f, which gives support to the far field acoustic results.

The screech frequency evolution in flight has been deduced from detailed near field acoustic signals. The prediction formula from Bryce & Pinker[14] has been investigated with particular expressions for the convection velocity whereas the flight effect on shock cell length has been modeled in following Morris.[1] For mode B and b, it was shown that the convection velocity estimate as $U_c = \alpha U_j$, with α being mode dependent, provided a very good frequency prediction. In particular, the slope of f_s with M_f was adequately estimated. This result gives support to the case of Sarohia & Massier[32] that the boundary layer on the outer wall of the model jet nozzle shields the supersonic jet from the secondary flow. Some frequency jumps have been observed while the flight Mach number M_f was increased. The screech mode evolution with M_f has been investigated from time signals for $M_j = 1.10$ and 1.50 and no frequency jump could be related to a screech azimuthal mode change. It does not mean that the screech was exactly identical on each side of a jump but only that the azimuthal instability mode related to screech remained unchanged across the observed discontinuities. Some work is still to be done to reveal the reason for the frequency jumps. It is believed that additional flow measurements, such as convective velocity measurements, should be able to further characterize and differentiate the screech modes arising from forward flight effects.

Acknowledgements

This research has been funded by the French Research Agency (Agence Nationale de la Recherche) through the ANR-10-BLAN-937-01 project JESSICA. The authors wish to express their most sincere thanks to Emmanuel Jondeau and Jean-Michel Perrin for their help in setting up the experiments.

References

[1]Morris, P. J., "A note on the effect of forward flight on shock spacing in circular jets," *Journal of Sound and Vibration*, Vol. 121, No. 1, 1988, pp. 175–177.

[2]Powell, A., "On the mechanism of choked jet noise," *Proceedings of the Physical Society of London*, Vol. 66, No. 408, 1953, pp. 1039–1056.

[3]Merle, M., "Sur la fréquence des ondes émises par un jet d'air à grande vitesse," Compte Rendu 243, Académie des sciences de Paris, 1956.

[4]Davies, M. G. and Oldfield, D. E. S., "Tones from a choked axisymmetric jet. I. Cell structure, eddy velocity and source locations," *Acustica*, Vol. 12, No. 4, 1962, pp. 257–266.

[5]Davies, M. G. and Oldfield, D. E. S., "Tones from a choked axisymmetric jet. II. The self excited loop and mode of oscillation," *Acustica*, Vol. 12, No. 4, 1962, pp. 267–277.

[6]Tam, C. K. W., Seiner, J. M., and Yu, J. C., "Proposed relationship between broadband shock associated noise and screech tones," *Journal of Sound and Vibration*, Vol. 110, No. 2, 1986, pp. 309–321.

[7]Powell, A., Umeda, Y., and Ishii, R., "Observations of the oscillation modes of choked circular jets," *Journal of the Acoustical Society of America*, Vol. 92, No. 5, 1992, pp. 2823–2836.

[8]Ponton, M. K. and Seiner, J. M., "Acoustic study of B helical mode for choked axisymmetric nozzle," *AIAA Journal*, Vol. 33, No. 3, 1995, pp. 413–419.

[9]Raman, G., "Advances in understanding supersonic jet screech : Review and perspective," *Progress in Aerospace Sciences*, Vol. 34, No. 1-2, 1998, pp. 45–106.

[10]Raman, G., "Supersonic jet screech: Half-century from Powell to the present," *Journal of Sound and Vibration*, Vol. 225, No. 3, 1999, pp. 543–571.

[11]Hay, J. A. and Rose, E. G., "In-flight shock cell noise," *Journal of Sound and Vibration*, Vol. 11, No. 4, 1970.

[12]Tam, C. K. W., "Jet noise generated by large-scale coherent motion," *Aeroacoustics of flight vehicles : theory and practice*, Vol. 1 : Noise sources, H. H. Hubbard (Ed.), 1991, pp. 311–390.

[13]Michalke, A. and Michel, U., "Prediction of jet noise in flight from static tests," *Journal of Sound and Vibration*, Vol. 67, No. 3, 1979, pp. 341–367.

[14]Bryce, W. D. and Pinker, R. A., "The noise from unheated supersonic jets in simulated flight," AIAA Paper 77-1327, 1977.

[15]Norum, T. D. and Shearin, J. G., "Effects of simulated flight on the structure and noise of underexpanded jets," NASA Technical Paper 2308, 1984.

[16]Krothapalli, A., Soderman, P. T., Allen, C. S., Hayes, J. A., and Jaeger, S. M., "Flight effects on the far-field noise of a heated supersonic jet," *AIAA Journal*, Vol. 35, No. 6, 1997.

[17]Norum, T. D. and Shearin, J. G., "Shock noise from supersonic jets in simulated flight to Mach 0.4," AIAA Paper 86-1945, 1986.

[18]Viswanathan, K. and Czech, M. J., "Measurement and modeling of effect of forward flight on jet noise," *AIAA Journal*, Vol. 49, No. 1, 2011, pp. 216–234.

[19]Brown, W. H., Ahuja, K. K., and Tam, C. K. W., "High speed flight effects on shock associated noise," AIAA Paper 86-1944, 1986.

[20]Norum, T. D. and Brown, M. C., "Simulated high speed flight effects on supersonic jet noise," AIAA Paper 93-4388, 1993.

[21]Anderson, J. D., *Modern compressible flow with historical perspective*, McGraw Hill, 2nd ed., 1990.

[22]Champagne, F. H. and Wygnanski, I. J., "An experimental investigation of coaxial turbulent jets," *International Journal of Heat and Mass Transfer*, Vol. 14, No. 9, 1971, pp. 1445–1464.

[23]Seiner, J. M. and Norum, T. D., "Aerodynamic aspects of shock containing jet plumes," AIAA Paper 80-0965, 1980.

[24]Viswanathan, K., "Best practices for accurate measurement of pure jet noise," *International Journal of Aeroacoustics*, Vol. 9, No. 1 & 2, 2010.

[25]Massey, K. C. and Ahuja, K. K., "Screech frequency prediction in light of mode detection and convection speed measurements for heated jets," AIAA Paper 97-1625, 1997.

[26]Plumblee, H. E., "Effects of forward velocity on turbulent jet mixing noise," NASA Contractor Report 2702, 1976.

[27]Morris, P. J., "Turbulence measurements in subsonic and supersonic axisymmetric jets in a parallel stream," *AIAA Journal*, Vol. 14, No. 10, 1976, pp. 1468–1475.

[28]Powell, A., "On Prandtl's formulas for supersonic jet cell length," *International Journal of Aeroacoustics*, Vol. 1 & 2, No. 9, 2010, pp. 207–236.

[29]Panda, J., Raman, G., and Zaman, K. B. M. Q., "Underexpanded screeching jets from circular, rectangular and elliptic nozzles," AIAA Paper 97-1623, 1997.

[30]Norum, T. D. and Shearin, J. G., "Shock structure and noise of supersonic jets in simulated flight to Mach 0.4," NASA Technical Paper 2785, 1988.

[31]Murakami, E. and Papamoschou, D., "Eddy convection in coaxial supersonic jets," *AIAA Journal*, Vol. 38, No. 4, 2000, pp. 628–635.

[32]Sarohia, V. and Massier, P. F., "Effects of external boundary-layer flow on jet noise in fight," *AIAA Journal*, Vol. 15, No. 5, 1977, pp. 659–664.

[33]Amiet, R. K., "Correction of open jet wind tunnel measurements for shear layer refraction," AIAA Paper 75-532, 1975.

[34]Amiet, R. K., "Refraction of sound by a shear layer," *Journal of Sound and Vibration*, Vol. 58, No. 4, 1978, pp. 467–482.

[35]Ahuja, K. K., Tanna, H. K., and Tester, B. J., "An experimental study of transmission, reflection and scattering of sound in a free jet flight simulation facility and comparison with theory," *Journal of Sound and Vibration*, Vol. 75, No. 1, 1981.

[36]Schlinker, R. H. and Amiet, R. K., "Shear layer refraction and scattering of sound," AIAA Paper 80-973, 1980.

[37]Sarohia, V., Parthasarathy, S. P., Massier, P. F., and Banerian, G., "Noise radiation from supersonic underexpanded jets in flight," AIAA Paper 80-1032, 1980.

[38]Sarohia, V., "Some flight simulation experiments on jet noise from supersonic underexpanded flows," *AIAA Journal*, Vol. 16, No. 7, 1978.

[39]André, B., Castelain, T., and Bailly, C., "Shock-tracking procedure for studying screech-induced oscillations," *Accepted for publication by AIAA Journal*.